

Evaluation of Corrosion Resistance of Thin Films 304 Stainless Steel Deposited by Sputtering

C. López-Meléndez^{1,2}, R.G. Bautista-Margulis³, E. M Garcia-Ochoa⁴, H. E. Esparza-Ponce¹, C. Carreño-Gallardo¹, C. Gaona-Tiburcio⁵, J. Uruchurtu-Chavarín⁶, A. Martínez-Villafañe^{1,*}

¹ Centro de Investigación en Materiales Avanzados, S.C. Miguel de Cervantes 120, Complejo Industrial Chihuahua C.P. 31109 Chihuahua, Chih. México

² Universidad La Salle Chihuahua. Prolongación Lomas de Majalca No. 11201 Col. Labor de Terrazas C.P. 31020 Chihuahua, Chih. México.

³ Universidad Juárez Autónoma de Tabasco, División Académica de Ciencias Biológicas, Villahermosa, Tab., 86040, México.

⁴ de Investigación en Corrosión (CICORR), Universidad Autónoma de Campeche, Av. A. Melgar s/n, Col. Buenavista, C.P. 24030 Campeche, Cam, Mexico.

⁵ Universidad Autónoma de Nuevo León. FIME - Centro de Innovación e Investigación en Ingeniería Aeronáutica. Av. Universidad s/n. Ciudad Universitaria. San Nicolás de los Garza, Nuevo León, México

⁶ Universidad Autónoma del Estado de Morelos-CIICAp Av. Universidad 1001, Col. Chamilpa, 62209-Cuernavaca Mor., México

*E-mail: martinez.villafane@cimav.edu.mx

Received: 30 November 2011 / Accepted: 4 January 2012 / Published: 1 February 2012

At present, new materials have been developed in the form of a thin film, due to the nanometer level improvement in the properties of bulk materials and this is increasingly important in materials science and engineering. In the present work, thin films of stainless steel 304 were grown in situ on substrate of the same material, with the technique of magnetron sputtering, three temperatures of deposit were varied: 25, 100 and 200°C, with the objective to reduce the particle size and increase resistance to corrosion. The films were microstructurally characterized by a) scanning electron microscope field emission to analyze the thickness of the film, b) atomic force microscopy to determine particle size and c) X-ray diffraction to obtain the phase analysis. The behavior to the corrosion was established by means of the techniques of potentiodynamic polarization curves and electrochemical noise. The results of the micrographs showed that the effect of the deposition temperature in the thin films (aids at reducing) the size of particle being minor to the conventional steel, homogenize the size with increasing temperature. The study of X-rays diffraction showed that as the temperature of the substratum increases the austenite phase is clearly defined. The results of Potentiodynamic polarization curves have allowed demonstrating that the films help in decreasing the corrosion susceptibility of this material. Likewise, the technique of electrochemical noise indicated the type of corrosion that it would be present in an aggressive environment such as sodium chloride showing corrosion pitting.

Keywords: 304 stainless steel, thin films, magnetron sputtering and corrosion

1. INTRODUCTION

Magnetron sputtering is one of the processes of physical vapor deposition (PVD) more important for growth of the thin films under vacuum conditions [1]. Recent research applies this technique to deposit nanostructured-films, improving corrosion resistance on the surface of the substrate [1-9]. The deposit for magnetron sputtering allows you to deposit a more uniform and stable coating free of dislocations, crystallography imperfections than other conventional methods [10]. Recently this technique has been applied to austenitic stainless steels which are very important in engineering since they possess a great chemical stability, in applications where a combination of high resistance is needed against corrosion, conformability and soldering [11], particularly for its excellent resistance to corrosion in aggressive environments [12]. Among these austenitic stainless steels lies the AISI 304 which shows very little resistance in a saline environment where it suffers severe localized corrosion [13]. Few research report the behavior to corrosion nanostructured films of this stainless steel on a substratum of the same steel, the electrochemical techniques as potentiodynamic polarization curves and electrochemical noise have been of great use to analyze the susceptibility to corrosion in different materials [14]. In this research work, it is evaluated the influence of a nanostructured film of AISI 304 on a substratum of the same material, in a corrosive environment of sodium chloride. The above mentioned film was prepared by the magnetron sputtering technique; the films were electrochemically exposed to evaluate its resistance to corrosion.

2. EXPERIMENTATION

2.1. Magnetron sputtering

The nanostructured films were prepared by magnetron sputtering, in a system of cathode erosion INTERCOVAMEX V3 with a source of direct pulsed current. The goal of this technique is to transport material from the target to a substrate via shooting ions towards the target by means of the argon gas, being accelerated by the high voltage [15]. The blank, obtained from the eroded atoms and the used substratum, came from the AISI 304. The composition of this material appears in the table 1.

Table 1. Chemical composition of 304 stainless steel (in wt.%)

C%	N%	Cr%	Ni%	Mn%	Si%	Fe%
0.026	0.067	17.756	7.770	1.377	0.370	Balance

The dimensions of the target are 76.2 mm of diameter per 1.59 mm of thickness, whilst the dimensions used for each specimen are 25X20X1.54 mm³. The substrates were previously prepared

before the deposit was refined superficially up to sandpaper #1000 of SiC and, subsequently, being cleaned by acetone in the ultrasound. The parameters for the deposit appear in table 2, where the experimental variable of interest was the temperature of deposit at three different temperatures 25, 10 and 200°C (three specimens were made for each temperature of deposit).

Table 2. Parameters of nanostructured films the AISI 304

Parameters	Specimens		
	1	2	3
Deposition temperature (°C)	25	100	200
Ar flow (sccm)	20	20	20
Deposition time (min)	30	30	30
Power (W)	100	100	100
Sputtering pressure(Pa)	2.53	2.53	2.53
Substrate	AISI 304		

After each deposit the films were characterized by X-ray diffraction (DRX) employing a diffractometer model Panalytical X'Pert Pro with detector X'Celerator using a Cu K α amp. The diffractograms were obtained using the following operating conditions: 30 to 120 degrees with a step of 0.05 degrees, 5 s/step and power 0.5 W to determinate the phase formed in each film. With the field emission scanning electron microscope model JSM-7401F (FESEM), the elementary composition and morphology was observed. Also, the size of particle or grain was observed by atomic force microscopy (AFM), using a VEECO SPM MultiMode for each one of the nanostructured films.

2.2. Electrochemical characterization

Table 3. Parameters for electrochemical techniques

Noise electrochemical		Potentiodynamic polarization curves	
Points	1024	scanning	± 600
Points/s	1	Scan rate	1 mV/s
Aqueous solution: NaCl 5% in wt Counter electrode: Platinum wire Reference electrode: Saturated calomel electrode (SCE)			

After having characterized each one of the nanostructured films, the resistance to the corrosion was analyzed by means of two electrochemical techniques: Potentiodynamic polarization curves with the objective of knowing the current density (i_{corr}), which was calculated by the Tafel's extrapolation method in a zone of ± 250 mV of the corrosion potential (E_{corr}), the potential of pitting (E_{pit}) and the potential of pitting nucleation (E_{np}), which were obtained from the average of three repetitions for each one of the analyzed specimens. For electrochemical noise, the measurements were performed in a

solartron 1285 potentiostat. Each of the thin films was subjected to an aggressive medium (sodium chloride to 5 % in weight), and the area exposed for each technique was 1 cm² at room temperature. Table 3 shows the parameters used for each of the applied techniques. The electrochemical cell for the immersion of each film used a cell of stung only to exhibit the zone of the film.

3. RESULTS

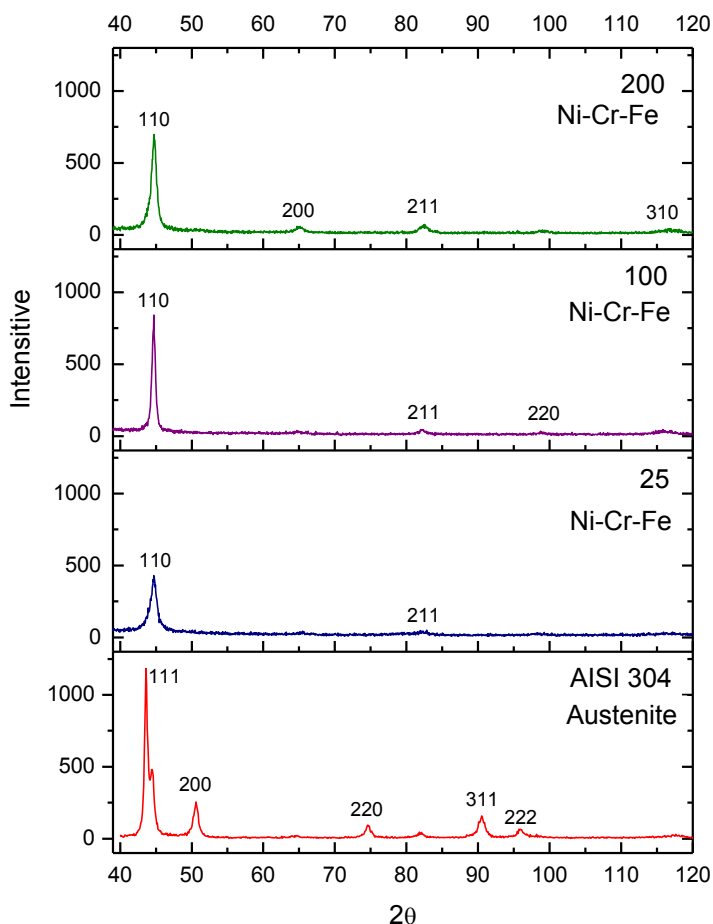


Figure 1. Diffraction patterns of AISI 304 and each of the nanostructured films.

Figure No. 1, shows the diffraction patterns of each of the films deposited at different temperatures and, for the AISI 304 substrate without film, the austenitic phase is present; while at temperatures of 25, 100 and 200°C, the films presented a Ni-Cr-Fe phase, observing a more defined austenite phase when increasing the substrate temperature. The thickness and adhesion of the films were analyzed by SEM. Figure No. 2 shows three images where the average thickness was about 200 nm. An optimal adhesion was not observed in figures 2a, 2b and 2c. Although there were good adhesion areas, some other areas did not show such adhesions due to the roughness of the substrate.

The specimens presented different morphology depending on the time of deposit. In Figure No. 3, it can be seen clusters of particles with an average size about 120 nm and particles smaller than

30 nm at 25°C; whereas Figure 3b shows how three-dimensional cracks in the substrate promote growth of the film, giving rise to the formation of agglomerates between 50 and 100 nm.

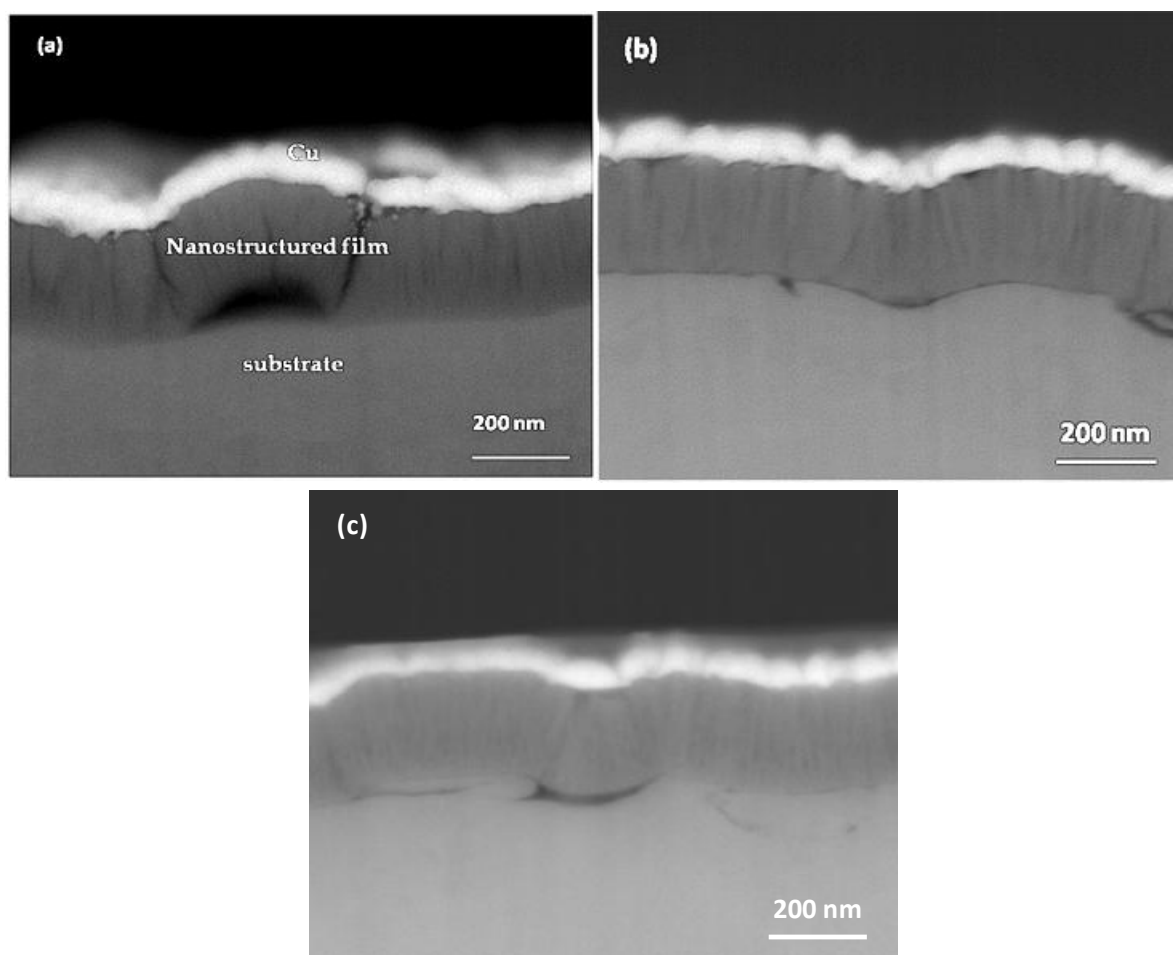


Figure 2. SEM Cross sectional morphology nanostructures films: (a) with temperature to deposited 25°C, (b) with temperature to deposited 100°C and (c) with temperature to deposited 200°C.

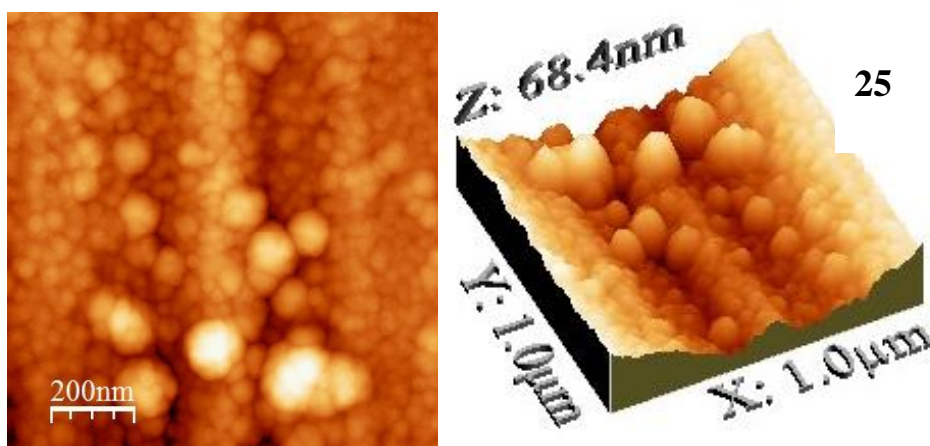


Figure 3. AFM image of a film with temperature to deposited of 25°C

Figure No. 4 shows the surface of the film deposited at 100°C, presenting a homogeneous growth without agglomerates with particle size below 50 nm. At 200°C, the particle size is on average 50 nm with a homogeneous surface without clusters (Figure 5). From this figure, it can also be seen a more defined formation of this structure as the temperature rises .

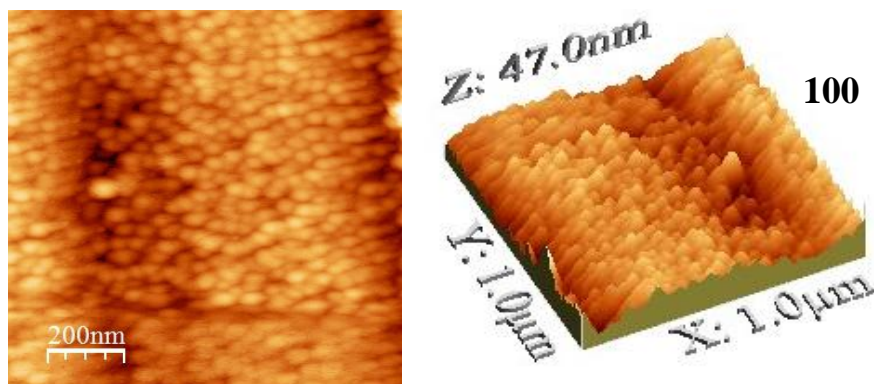


Figure 4. AFM image of a film with temperature to deposited of 100°C.

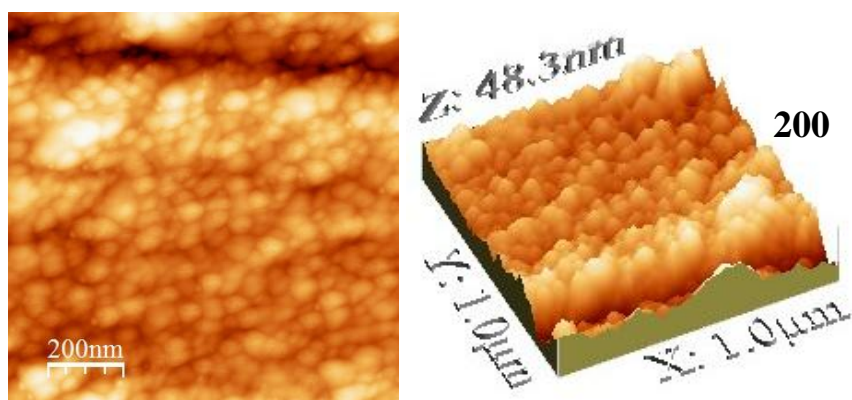


Figure 5. AFM image of a film with temperature to deposited of 200°C.

In the films deposited at room temperature, the presence of agglomerates is evident. More grip and arrangement of atoms (100°C) were observed as the temperature increased. At 200°C temperature, a homogeneous distribution and a slight increase in particle size was found. At low temperature a Stranky-Krastanov growth type was observed.

Stranky atoms initially form complete monolayer films on the substrate and after several monolayer islands starts growing on these layers. For temperatures of 100 and 200°C, the rate of growth is more like the Frank-Van der Merwe type, where the force of attraction between the substrate and adsorbed atoms is stronger than the bonds between the atoms, due to heating of the substrate.

3.1. Electrochemical tests

Figure No.6 shows the potentiodynamic polarization curves of each of the films and AISI304 without film, showing a passivation-activation system. In AISI304 there is a characteristic curve of this material in the corrosion potential (E_{corr}) of the films. There is also a potential nobler than the material without this film, being more susceptible to corrosion.

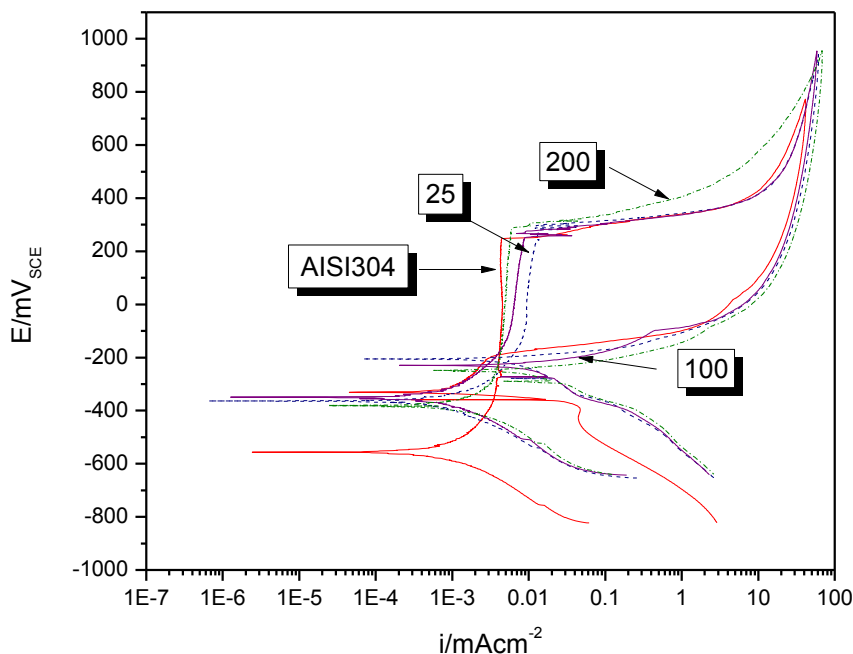


Figure 6. Potentiodynamic polarization curves of the AISI304 without film and the different nanostructured-film temperature of the deposit.

Table 4. Data obtained from the potentiodynamic polarization curves

Specimens	E_{corr} (mV)	E_{pit} (mV)	E_{np} (mV)	i_{corr} ($mAcm^{-2}$)
Bulk	-554.67	-189.51	248.09	8.277E-4
25	-363.64	-196.71	278.68	6.417E-4
100	-346.59	-225.95	251.54	6.102E-4
200	-379.41	-243.49	287.23	1.593E-3

Table No. 4 shows the data obtained from the potentiodynamic polarization curves that present the AISI304 steel without film and each of the films in the potential of pitting (E_{pit}), showing that increasing the substrate E_{pit} temperature increases more than the base material. The potential for pitting nucleation (E_{np}) was observed to vary without having a sequence with respect to the temperature increase of the deposit. Passivation was present in all films; however, at 200°C

deposition temperature more activation was shown in the current density (i_{corr}) than those at 25 and 200°C.

The analysis of electrochemical noise technique was carried out from the data obtained from the films, eliminating thus their tendency. The time series shown in figure 7 illustrate the time series - potential visual analysis. In this figure 7, it can be seen that the behavior of the stainless steel, in the presence of NaCl, showed activity in the first 200 seconds giving enough time for the formation of a passive layer and presenting a breakdown later on; while the current-time series in figure 8 showed the characteristic activity of active-passive material.

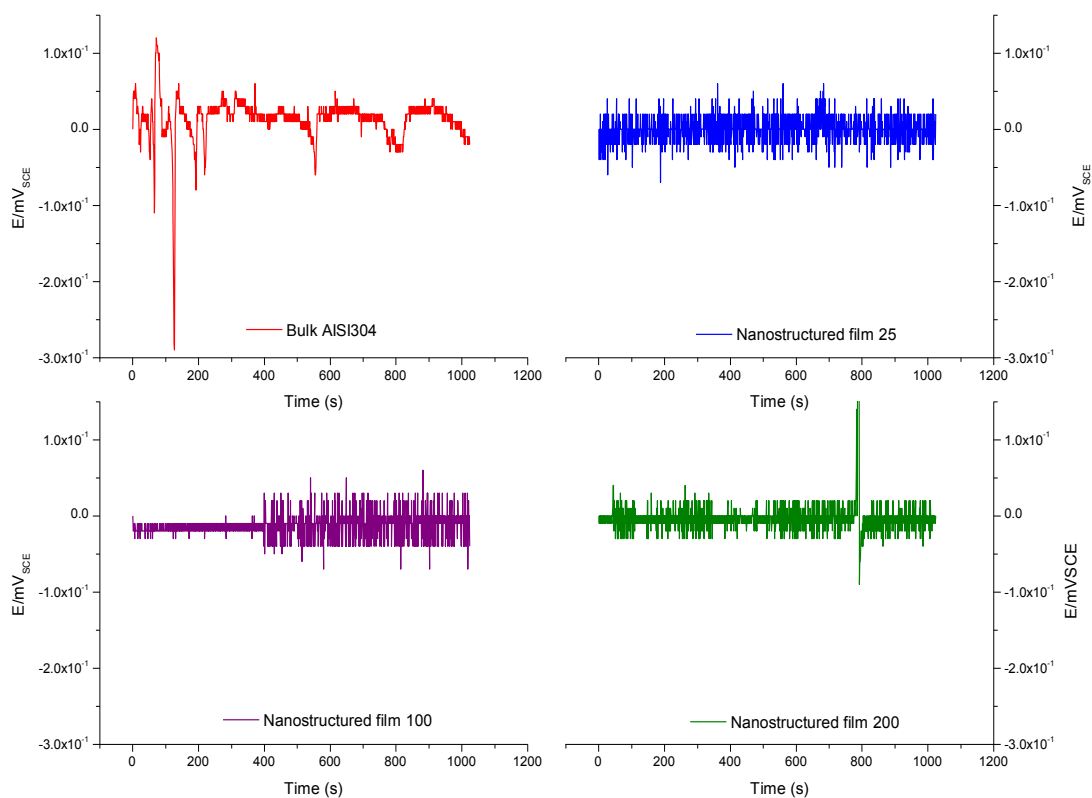


Figure 7. Noise in voltage for AISI304 and the different nanostructured films 25, 100 and 200°C.

Figure 7, shows the coating which was deposited at 25°C, indicating a potential time series with stable transient repassivation and breakdown; while on-stream time series (figure 8 at 25°C) was found to be very active in comparison with coatings of 100 and 200°C with amplitudes of -4×10^{-4} to 4×10^{-4} $mAcm^{-2}$. This might be related to the heterogeneity of the film deposit. At 100°C, the film deposited showed stability during approximately 400s in the time series-potential. Afterwards, there was more activation with localized corrosion due to a low activity in the time series-current (figure 8 at 100 °C). A comparison made with the nanostructured film at 200°C, it did show activation in the series showing a repetitive behavior in the activation-passivation (figure 7 at 200°C).

Figure 10 shows the behavior of the noise resistance of AISI304 without film and each of the nanostructured films. The film resistance was observed to increase at 100 and 200°C, showing greater resistance at 100°C than the other two films. At 25°C, the film presented a similar resistance to AISI 304. The impedance spectrum of current noise is shown in Figure 9.

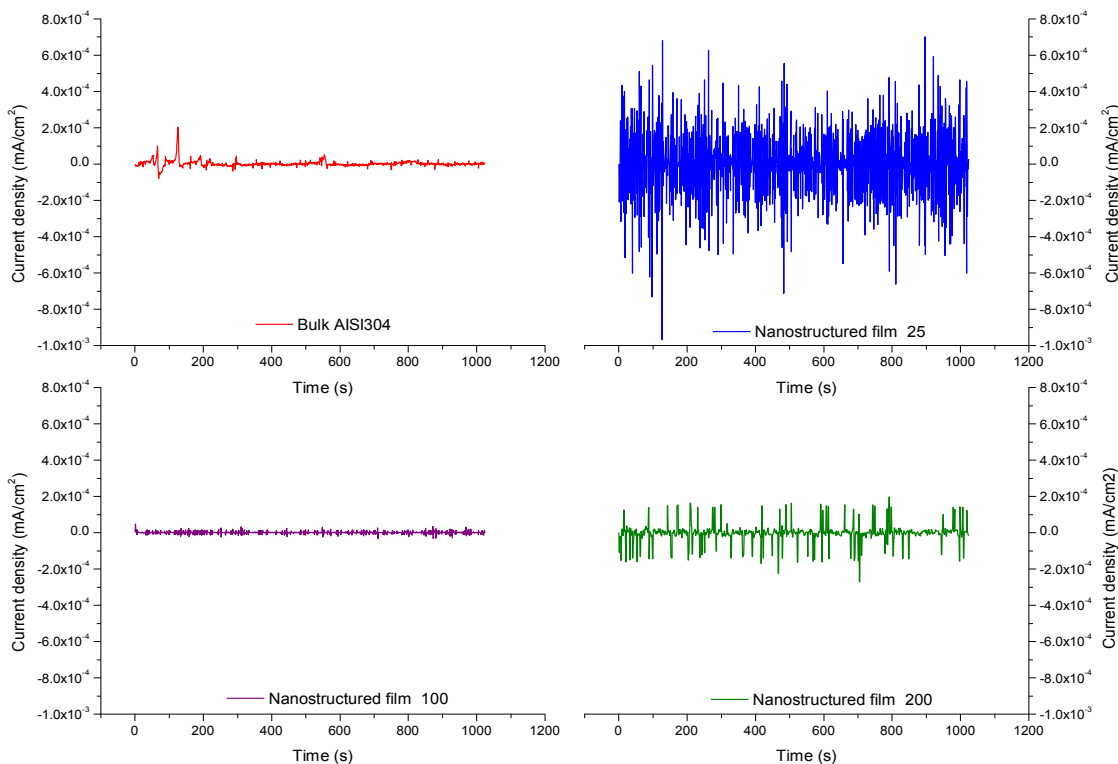


Figure 8. Noise in current for AISI304 and the different nanostructured films 25, 100 and 200°C.

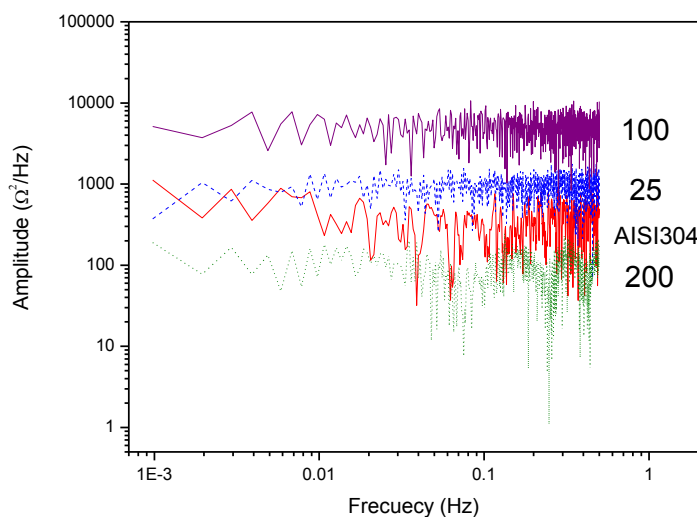


Figure 9. Noise spectral impedance in current for AISI304 and the different nanostructured films 25, 100 and 200°C.

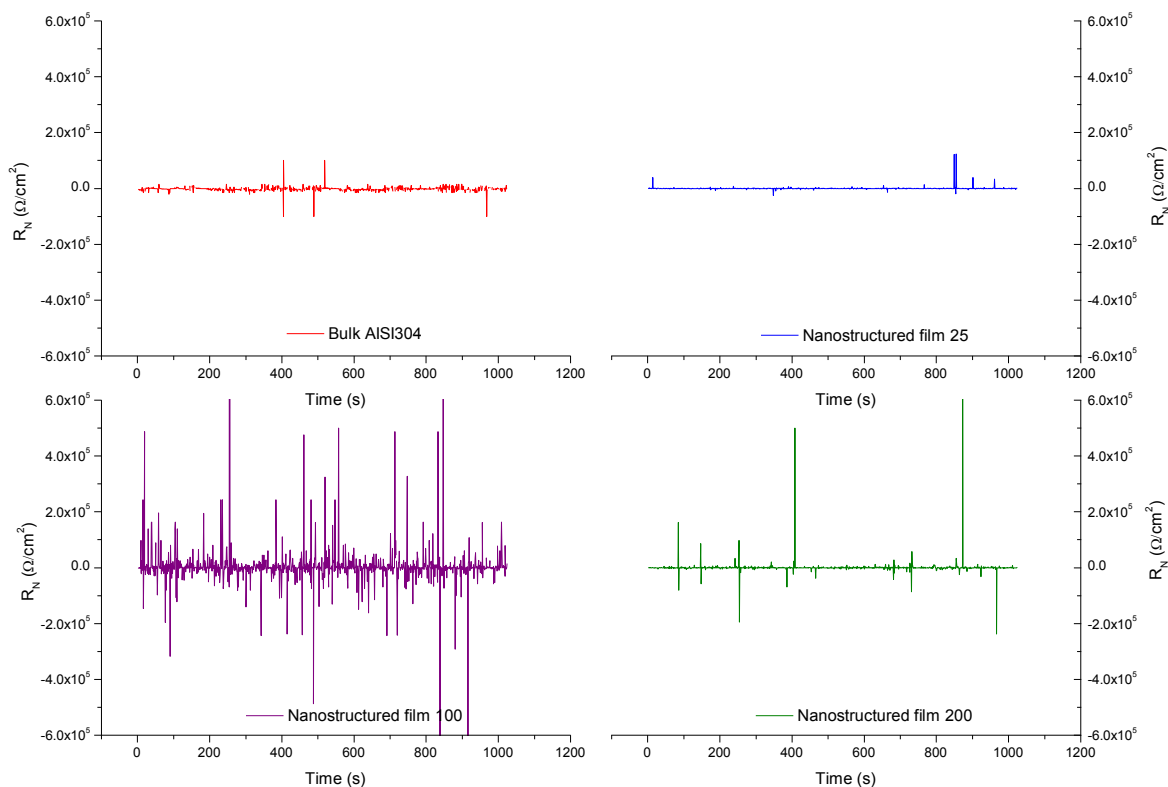


Figure 10. Noise resistance of the AISI304 and the different nanostructured films 25, 100 and 200°C.

Table 5. Localization index for the analyzed nanostructured films

Specimen	Localization index	Corrosion type
AISI 304	0.0346	mixed
25	0.3211	located
100	0.1360	located
200	0.1490	located

Table 5 shows the location index for each of the specimens showing a higher rate of localization in the nanostructured films at 25, 100 and 200 °C.

4. CONCLUSIONS

For the studied coatings, the temperature of deposition influenced the formation of microstructure, showing a homogeneous growth on the surface of the substrate at 100 °C. At this temperature, electrochemical techniques with potentiodynamic curves and electrochemical noise were found to increase the corrosion resistance, compared to the other two substrate temperatures of 25 and 200 °C, exposed in an aqueous medium of 5% NaCl by

weight. Therefore, the particle size reduction of the coating can be an effective method to increase corrosion resistance in this type of stainless steel.

ACKNOWLEDGMENTS

This work was supported by Nanomining-263942 (FP7-NMP-2010-EU-MEXICO). The technical assistance by Adan Borunda, Victor Orozco, Enrique Torres, Wilbert Antunez, Jair Lugo Cuevas, Carlos Ornelas and Oscar Solis is gratefully acknowledged.

References

1. B. window, *Surf. Coat. Technol.*, 71 (1995) 93-97
2. Guozhe Meng, Ying Li, Fuhui Wang, *Electrochimica Acta*, 51 (2005) 4277-4284
3. XI Yan-jun, LU Jin-bin, WANG Zhi-xin, HE Lian-long, WANG Fu-hui, *Transactions of Nonferrous Metals Society of China*, 16 (2005) 511-516
4. Min Ku Lee, Whung Whoe Kim, Joung Soo Kim, Won Jong Lee, *J. Nuclear Mater.*, 254 (1999) 42-48.
5. S.A.M. Refaey, F. Taha, A.M. Abd El-Malak, *Int. J. Electrochem. Sci.* 1 (2006) 80
6. V.B. Singh, M. Ray, *Int. J. Electrochem. Sci.* 2 (2007) 329
7. H.H. Hassan, K. Fahmy, *Int. J. Electrochem. Sci.* 3 (2008) 29
8. Hai-Bo Lu, Ying Li, Fu-Hui Wang, *Thin Solid Films*, 510 (2006) 197-202
9. M. Flores, L. Huerta, R. Escamilla, E. Andrade, S. Muhl, *Appl. Surf. Sci.*, 253(2007) 7192-7196
10. Konstantinas Leinartas, Meilute Samuleviciene, Audrius Bagdonas, Remigijus Juskenas and Eimutis Juzeliuna, *Surf. Coat. Technol.*, 168 (2003) 70-77
11. ASM Handbook, *Properties and Selection: Irons, Steels, and High Performance Alloy*, American Society of Metals, Vol. 1, 10th Edition, (1993)
12. Morteza Zandrahimi, M. Reza Bateni, A. Poladi, Jerzy A. Szpunar, *Wear*, 263 (2007) 674-678
13. Yanhua Wang, Wei Wang, Yuanyuan Liu, Lian Zhong and Jia Wang, *Corr. Sci.*, 53 (2011) 2963-2968
14. I. E. Castañeda, J.G. Gonzalez-Rodriguez, G. Dominguez-Patiño, R. Sandoval-Jabalera, M.A.Neri-Flores, JG. Chacon-Nava, A. Martinez-Villafañe, *Int. J. Electrochem. Sci.*, 6 (2011) 404-418
15. ASM Handbook, *Corrosion*, Vol. 13 (1996) 759